OCT 22 1996
Sta. 37 (20)

ENGINEERING DATA TRANSMITTAL

1. EDT 619216

2. To: (Receiving Organization) Distribution	3. From: (Originating Organization) Criticality and Shielding	4. Related EDT No.: 619216
5. Proj./Prog./Dept./Div.: 8M720	6. Design Authority/ Design Agent/Cog. Engr.: W. D. Wittekind	7. Purchase Order No.: NA
8. Originator Remarks: Approval/Release		9. Equip./Component No.: NA
		10. System/Bldg./Facility:
11. Receiver Remarks: 11A. Design Baseline Document? [X] Yes [] No (WDW)		12. Major Assm. Dwg. No.: NA
		13. Permit/Permit Application No.: NA
		14. Required Response Date:

15. DATA TRANSMITTED

(A) Item No.	(B) Document/Drawing No.	(C) Sheet No.	(D) Rev. No.	(E) Title or Description of Data Transmitted	(F) Approval Designator	(G) Reason for Transmittal	(H) Originator Disposition	(I) Receiver Disposition
1.	WHC-SD-WM-ER-619		0	Surface Moisture Measurement System Electromagnetic Induction Probe Surface Irregularity Tests	NA	1/2		

16. KEY

Approval Designator (F)	Reason for Transmittal (G)	Disposition (H) & (I)
E, S, Q, D or N/A (see WHC-CM-3-5, Sec.12.7)	1. Approval 2. Release 3. Information 4. Review 5. Post-Review 6. Dist. (Receipt Acknow. Required)	1. Approved 2. Approved w/comment 3. Disapproved w/comment 4. Reviewed no/comment 5. Reviewed w/comment 6. Receipt acknowledged

17. SIGNATURE/DISTRIBUTION
(See Approval Designator for required signatures)

(G) Reason	(H) Disp.	(J) Name (K) Signature (L) Date (M) MSIN	(G) Reason	(H) Disp.	(J) Name (K) Signature (L) Date (M) MSIN
1	1	Design Authority [signature] 10/22/96	1	1	D. L. Lessor [signature] 10-15-96
		Design Agent			
1	1	Cog.Eng. W. D. Wittekind [signature] 14/10/96			
1	1	Cog. Mgr. J. Greenborg [signature] 10/15/96			
		QA			
		Safety			
		Env.			

18. W. D. Wittekind [signature] 14 OCT. 1996 Signature of EDT Originator Date	19. G. F. Vargo, Jr [signature] Authorized Representative for Receiving Organization Date	20. J. Greenborg [signature] 10/15/96 Design Authority/ Cognizant Manager Date	21. DOE APPROVAL (if required) Ctrl. No. [] Approved [] Approved w/comments [] Disapproved w/comments

Surface Moisture Measurement System Electromagnetic Induction Probe Surface Irregularity Tests

W. D. Wittekind
Westinghouse Hanford Company, Richland, WA 99352
U.S. Department of Energy Contract DE-AC06-87RL10930

EDT/ECN: 619216 UC: 606
Org Code: ~~403~~ 8M720 Charge Code: N2210
B&R Code: ~~1N23E40501~~ EW3120072 Total Pages: 30
Key Words: EMI, electromagnetic induction, moisture measurements, HLW tanks

Abstract: Surface irregularities cause the EMI moisture measurement to infer too low of a free water content in the HLW tank.

Janis Bishop 10-22-96
Release Approval Date

OCT 22 1996
DATE:
STA: 37
HANFORD RELEASE
ID: 29
Release Stamp

Approved for Public Release

SURFACE MOISTURE MEASUREMENT SYSTEM ELECTROMAGNETIC INDUCTION PROBE SURFACE IRREGULARITY TESTS

Warren D. Wittekind

Westinghouse Hanford Company
Richland, Washington

ABSTRACT

Surface Irregularity Tests

The surface of waste tank contents is irregular; the salt cake may have cracks, voids, humps and dips, etc. These surface irregularities have some effect on the free water content of the waste medium inferred from the electromagnetic induction (EMI) signal.

Several experimental tests were performed on liquids of known electrical conductivity with a wide side-to-side not electrically conducting void centered directly underneath the EMI test coil. This inhomogeneity geometry was chosen because it was believed to be the worst case void for the EMI technique in that the greatest fraction of the circular induced currents would be disrupted by this shape.

The inhomogeneity test results are consistent with the electrically non-conducting voids reducing the effective medium conductivity. The EMI signal reduction and hence the reduction in the inferred conductivity is almost linear with the void fraction from inhomogeneities uniform in depth.

The consequence of reducing the effective medium conductivity is that the EMI inferred free water content represents a lower limit for the free water content. Greater void inhomogeneities would cause a greater EMI underestimate of the free water content actually present. The effect of reducing medium conductivity on EMI inferred free water content is non-linear. A uniform 5% void inhomogeneity would cause an EMI underestimate of the free water content by approximately 2%, a uniform 10% void inhomogeneity would cause an EMI underestimate of the free water content by approximately 4%, a uniform 25% void inhomogeneity would cause an EMI underestimate of the free water content by approximately 12%, and a uniform 50% void inhomogeneity would cause an EMI underestimate of the free water content by approximately 31%.

Void inhomogeneities that are not uniform in depth but that are concentrated in regions of higher electromagnetic fields, that is closer to the EMI coils, will cause a disproportionately greater EMI underestimate of the free water content.

CONTENTS

LIST OF FIGURES

LIST OF TABLES

1.0 INTRODUCTION

This report documents laboratory measurements to infer the effect of surface inhomogeneities on EMI determined moisture content.

The electromagnetic induction (EMI) probe is being developed by WHC (Crowe and Wittekind 1995) to measure the amount of water remaining in waste stored in the high-level waste tanks on the Hanford Site. A previous report (Wittekind and Crowe, 1996) considered the medium moisture content relationship to medium electrical conductivity. Another report (Wittekind and Crowe, et.al. 1996) considered the EMI signal relationship to medium electrical conductivity.

The electromagnetic probe uses a magnetic field to induce electrical current in the surrounding waste proportional to the waste conductivity. The moisture content of the waste is estimated based on the measured waste conductivity. The EMI coil measured signal amplitude is proportional to the waste electrical conductivity.

2.0 SUMMARY

2.1 Purpose

This report provides details about EMI work in progress. Descriptions are given of:

- EMI operating hardware, and
- Experimental EMI measurements on the effect of surface inhomogeneities.

The EMI probe response was measured with medium conductivities of 0 mS/cm, 5 mS/cm, 10 mS/cm, 20 mS/cm, and 40 mS/cm. The inhomogeneity test pieces consisted of the "W" part of standard length and width, the "X" piece with a greater depth, and the "Y" piece with a narrower width. This allowed one variation in inhomogeneity depth and one variation in inhomogeneity width.

EMI measurements were performed on conductivity test standards with the solution electrical conductivity determined using the standard techniques of an electrical conductivity meter and purchased standard solutions.

2.2 Conclusion

Inhomogeneity data is consistent with reduction of EMI signal amplitude proportional to the reduction of the effective volume contributing to the sample electrical conductivity. It is assumed that inhomogeneities are nonconducting inhomogeneities and diminish the total electrically conducting volume. There was not adequate data to define the depth effect, but this is expected to be consistent with EMI depth sensitivity.

Another way to state this conclusion is that the EMI signal amplitude is proportional to the effective volume fraction of the medium available to contribute to electrical conductivity. That is in the solid medium volume with the void inhomogeneities, the space occupied by voids does not contribute to sample electrical conductivity. The final effect is that the EMI inferred moisture content will be lower than the actual moisture content due to the presence of void inhomogeneities.

3.0 EMI MEASUREMENT SYSTEM DESCRIPTION

3.1 EMI Operating Hardware

An EMI moisture monitor for assaying the effective average free water moisture content in solid salt cake material has been assembled and tested. The two main components are: (1) an eddy current tester (Model MIZ-40A manufactured by ZETEC of Issaquah, Washington), and (2) a custom designed coil pair for this application. There is an electrical intrinsic safety barrier between the MIZ-40A and the EMI coils for safe operation in a hazardous atmosphere. Additional components necessary to record EMI data on archival medium include analog-to-digital converters, and position encoders.

3.2 Components

The EMI probe circuit, starting at the MIZ-40A, has the successive components of 1) MIZ-40A eddy current tester, 2) coaxial cables approximately 100 ft long (two RG 174/U or equivalent), 3) dual channel intrinsic safety barrier (ISB) for ±9 volts (167 Ω ISB number 9002/22-240-160-00), alternating current, 4) coaxial cables for deployment into a hazardous environment, 5) two EMI coils for electrical conductivity sensing.

3.3 Configuration

3.3.1 EMI Coil Configuration

The EMI coil has the pancake geometry. The pancake geometry puts the coils into a plane of relatively small thickness with significant difference between the inside diameter and the outside diameter. The coil, with associated coaxial cables and intrinsic safety barrier (ISB) is designed to operate at 400 khz. Approximately 85 feet of additional coaxial cable between the van and the ISB has reduced the effective resonance to approximately 360 khz. The 400 khz coil housing has an outside diameter of 3 inches. The coil has an inside diameter of 2.10 inches. There are 23 turns of AWG 20 gauge wire. The reported inductance of this coil is 55 μH.

3.3.2 EMI Probe Configuration

The EMI probe length is 12 3/8 in. and the EMI probe diameter, 3.5 in., is consistent with the requirements for entering the HLW tank vapor space through a 4 inch carbon steel pipe used for a riser.

The EMI coil configuration uses two coils separated by 5 in. The 5 inch coil spacing allows a tungsten weight to be placed approximately 4 inches away within the EMI probe housing. The tungsten weight will bring the total weight of the EMI probe up to 25 lbs. This weight was found to be necessary for the probe to pull the electrical cable from the take up reel when being deployed.

The EMI probe housing is an electrically conducting high density polyethylene. The polyethylene was made electrically conducting by adding graphite into the polyethylene by the plastic supplier. It is believed that the semi-conducting plastic will dissipate static electrical charges.

The two EMI coils were designed for a resonant frequency of 400 khz, and operate in the test/reference mode, with the frequencies of operation expected to be between 200 and 500 khz

The EMI probe size and total weight is not much different than neutron moisture monitoring probe. The EMI probe is electrically simpler than the neutron moisture monitoring probe and does not require an explosion proof housing.

3.3.3 EMI Probe Circuit

The EMI probe circuit, beginning at the MIZ-40A includes coaxial cable connections to the intrinsic safety barrier (ISB), the intrinsic safety barrier, and additional coaxial cable connections inside the HLW tank that connect to the EMI coils, and finally the 400 khz coils.

There is a mercury-wetted slip ring in the circuit between the ISB and the coaxial cable to the EMI coil. This allows an electrical connection while a spool with the coaxial cable turns to lower the coil to the electrically conductive surface.

The ISB is R. Stahl Inc.'s INTRINSPAK 9002/22-240-160-00. This is a dual channel ISB designed for alternating current ±9 V. There is a 167 Ω resistor, which permits intrinsically safe operation in a Class I, Group B (hydrogen atmosphere or equal) with an inductor as large as 6.5 mH.

The coaxial cable shields are grounded at the ISB. Since the center conductor of the coaxial cable was connected through the ISB, it would be redundant to connect the shield of the coaxial cable through the ISB also.

There is approximately 100 feet of SMMS cable (equivalent to RG 174 coaxial cable) between the EMI coil and the ISB. There is approximately another 85 feet of SMMS cable between the ISB and the MIZ-40A eddy current tester.

The MIZ-40A is an eddy current tester designed for use around nuclear plants for balance of plant operation. The MIZ-40A can sample EMI coil signal response at four frequencies simultaneously. There are analog electrical outputs available that allow connection to an analog to digital convertor and eventual long term storage media.

3.4 EMI Probe Medium Conductivity Response

The EMI probe operates on an inductive effect. There are two EMI coils, 5 inches apart, the absolute is on the bottom while the reference coil is on the top and remote from the medium being interrogated. There is a change in inductance in one coil when it is close to an electrically conductive medium. The MIZ-40A eddy current tester subtracts the EMI response of the reference coil from the EMI response of the absolute coil, the difference is the EMI signal. The greater the electrical conductivity of the medium being interrogated, the greater will be the induced electrical current in the conducting and consequently the greater will be the change in magnetic field at the absolute coil location.

Figure 1., Surface Moisture Monitor EMI Probe, shows the arrangement of the two EMI coils inside the EMI probe housing.

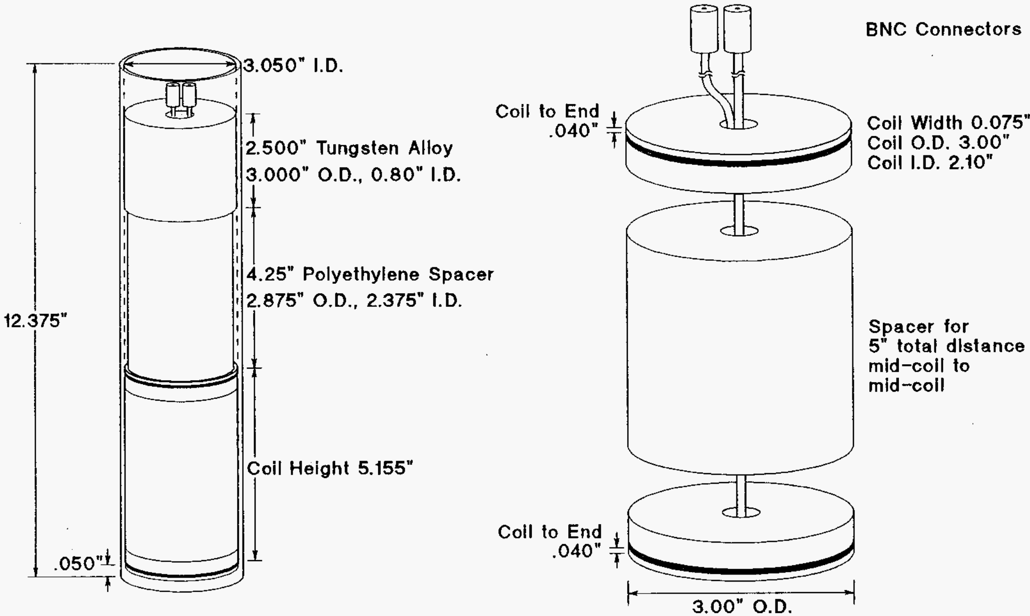

Surface Moisture Monitor EMI Probe

Matched coils on separate spool pieces with 8" to 10" of coaxial cable and BNC connector.

Spacer with center clearance for BNC connector.

Semiconducting polyethylene cylinder with 0.050" thickness at tip.

Figure 1. Surface Moisture Monitor EMI Probe

Figure 2. EMI Surface Irregularity Attachment

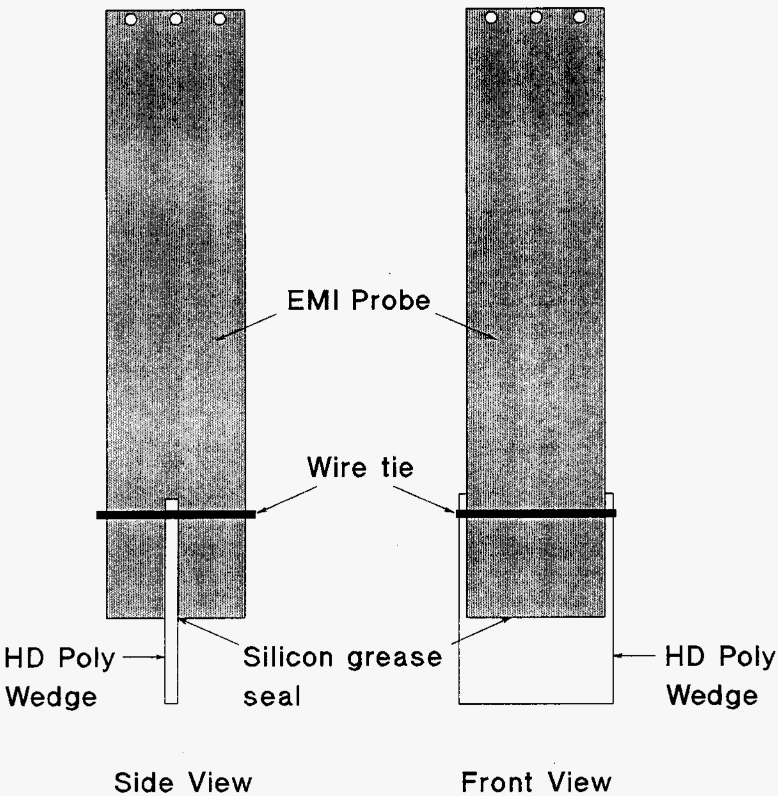

EMI Surface Irregularity Attachment

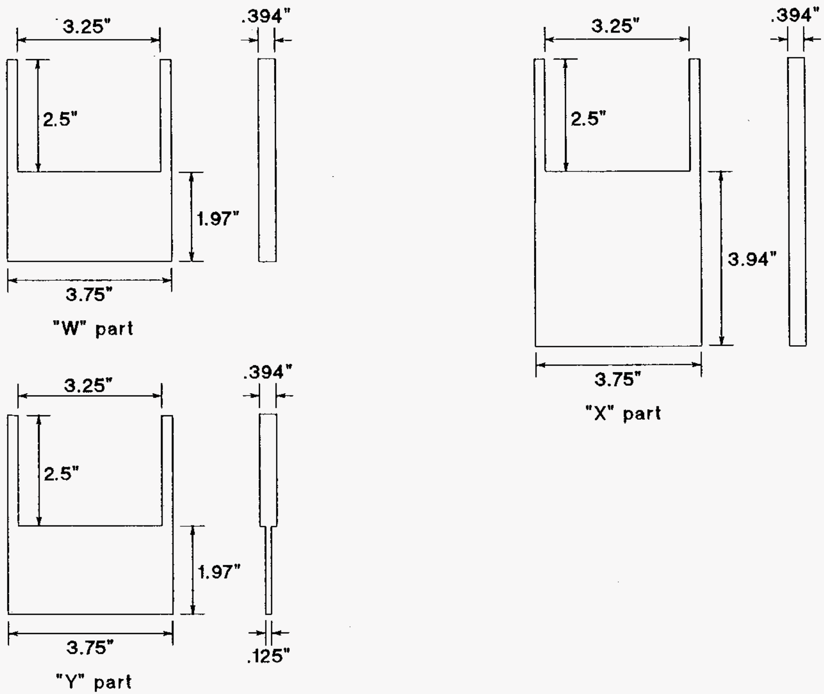

EMI Surface Irregularity Test Pieces

"W" is a standard inhomogeniety model. "X" has increased depth. "Y" has decreased width.

WDW358

Figure 3. EMI Surface Irregularity Test Pieces

4.0 SURFACE INHOMOGENEITY TESTING

The surface inhomogeneity was created in the electrically conducting liquid by attaching nonconducting plastic forms to the EMI probe. Figure 2., EMI Surface Irregularity Attachment, shows the attachment of the plastic form to the EMI probe housing. Figure 3, EMI Surface Irregularity Test Pieces shows three different plastic forms used to create surface irregularities. The three forms allow for one standard surface inhomogeneity, one variation in thickness, and one variation in depth.

EMI Probe Laboratory Surface Inhomogeneity Test Performed:

Date: 12 August 1996
Series: Surface Inhomogeneity Tests
Probe: 400 khz Zetec Coils, 5 inch coil spacing
Probe: Polyethylene with graphite (under 10^6 Ohm-cm resistivity)
Values: 320 khz, 340 khz, and 360 khz.
Values: 0 mS/cm, 05 mS/cm, 10 mS/cm, 20 mS/cm, and 40 mS/cm.
Values: Three surface inhomogeneities (W, X and Y) and none.
Values: W and X have same widths, X part is twice depth of W.
Values: W and Y have same depths, Y part is half width of W.
Results: EMI signal variation with inhomogeneity.
Observations: 1) 0 mS/cm: none & X similar, W & Y lower.
Observations: 2) 5 mS/cm: none & X similar, W & Y lower.
Observations: 3) 10 mS/cm: none, W & X similar, Y lower.
Observations: 4) 20 mS/cm: none is highest, Y, X & W lower.
Observations: 5) 40 mS/cm: none is highest, Y, X & W lower.
CONCLUSIONS:
A) EMI amplitude trend is consistent that greater width of inhomogeneity causes a lower EMI signal.
B) EMI amplitude trend is not definitive that depth of inhomogeneity causes a lower EMI signal.
C) EMI amplitude is consistent with the inhomogeneity causing a lower EMI signal.
D) EMI amplitude is most consistent with the scan starting distance causing a variation in EMI signal amplitude. This is the same as saying that just where the EMI probe is "zeroed" for a reference point is significant and that it should be remote from the surface being interrogated.

5.0 INTERPRETATION OF RESULTS

5.1 Surface Inhomogeneity Measurement Prediction

The sensitivity region of the pancake shape of the EMI coil with a 0.075 inch thickness and diameters of 3.0 inches O.D. and 2.1 inches I.D. can be expected to be focussed down, with reduced sensitivity off to the side.

Because of the homogeneous shape of the coil with approximately 2 layers of turns between the coil bottom and coil top, EMI signal from samples with inhomogeneities can be expected to depend more on total sample volume and less on the specific arrangement of the surface inhomogeneity. This statement must be qualified because volumes closer to the EMI coils are where electromagnetic fields are stronger and count more heavily than volumes that are more remote from the EMI coils and are where electromagnetic fields are weaker.

The quantitative reduction of EMI signal amplitude from non-conducting inhomogeneities could be estimated by the ratio of sample volume without inhomogeneities to the total volume of the sample volume with the void inhomogeneities.

The quantitative effect on EMI signal phase of the surface inhomogeneity is expected to be zero. A phase shift could be introduced by a change in EMI probe capacitance, but the electrically conducting EMI coil housing short circuits the probe capacitance, eliminating the cause of phase shift.

EMI depth of penetration with 90% of the signal coming from approximately the first 3 inches of depth, was not expected to show much variation between the 1.97 inch depth test pieces (W and Y parts), and the 3.94 inch depth test piece (X part).

5.1.1 Surface Inhomogeneity Theoretical Calculation

A theoretical calculations of the effect of electrically conducting flaws on the signal amplitude was performed by Burrows (Burrows, 1964). There were four cases considered:

1) prolate spheroid, field parallel long axis,
2) prolate spheroid, field perpendicular long axis,
3) oblate spheroid, field parallel short axis, and
4) oblate spheroid, field perpendicular short axis.

A prolate spheroid is a shape between a sphere and a rod; one axis is long and the two equal axes are short. An oblate spheroid is a shape between a sphere and a circular disk; one axis is short and the two equal axes are long.

The base case is the non-conducting sphere, where P_0, induced dipole moment, (Burroughs, 1964, Equations 5.5, 5.10 and 7.14) is:

$$\overline{P_0} = -\frac{3}{2} V \overline{j_i}$$

where
V is the volume of the sphere, and
j_i is the average current density.

For the special case of a non-conducting long rod in a parallel field, the induced dipole approaches the limiting value:

$$\overline{P_L} = \alpha_L \overline{P_0} = \frac{2}{3} \overline{P_0}$$

For the special case of a non-conducting long rod in a transverse field, the induced dipole approaches the limiting value:

$$\overline{P_T} = \alpha_T \overline{P_0} = \frac{4}{3} \overline{P_0}$$

For the special case of a non-conducting flat disk in a parallel field, the induced dipole approaches the limiting value:

$$\overline{P_L} = \alpha_L \overline{P_0} = \frac{4\ b}{3\ \pi\ a} \overline{P_0}$$

where
a is the length of the short axis, and
b is the length of the two long axes.

For the special case of a non-conducting flat disk in a transverse field, the induced dipole approaches the limiting value:

$$\overline{P_T} = \alpha_T \overline{P_0} = \frac{2}{3} \overline{P_0}$$

5.1.2 Surface Inhomogeneity Theoretical Discussion

The calculations from Burrows (Burrows, 1964) had assumed a constant electrical field with different shapes of nonconducting voids introduced in the path of this constant electrical field. The magnetic field produced by the pancake geometry EMI coil leads to an circular or azimuthal current flow. When nonconducting obstacles are placed in this current flow, the current simply deviates around the obstacle and flows according to the path of least resistance. This situation leads to an electrical current flow that would be parallel the void inhomogeneity surface instead of perpendicular to it. Electrical current flow perpendicular to the nonconducting obstacle would be a path of greater resistance. The coefficient for the prolate spheroid with an electrical field parallel the prolate spheroid surface has the limiting value of $\alpha_L = 2/3$. The coefficient for the oblate spheroid with an electrical field parallel the oblate spheroid surface has the limiting value of $\alpha_T = 2/3$. This 2/3 factor times the dipole moment for an equivalent volume sphere, which has a 3/2 factor, leads to EMI signal reduction, P_F, directly proportional to the product of volume and current density:

$$\overline{P_F} = \alpha \overline{P_0} = \frac{2}{3} \overline{P_0} = \frac{2}{3}\left(-\frac{3}{2} V \overline{J_i}\right) = -V \overline{J_i}$$

where
V is the inhomogeneity volume with current parallel the surface, and
j_i is the average current density.

There is the assumption that the void inhomogeneity was subject to the same current field that the bulk volume was subject to. This means that the current term can be canceled out. The fractional diminishment of EMI signal amplitude for a nonconducting void inhomogeneity with current flow parallel the surface is calculated from

$$EMI\ Signal\ Fraction = \frac{\overline{P} - \overline{P_F}}{\overline{P}} = \frac{(\pi/4)a^2L - taL}{(\pi/4)a^2L} = \frac{(\pi/4)a - t}{(\pi/4)a}$$

where
a is the diameter of a cylinder of sample below EMI coil,
L is the effective depth of EMI penetration, and
t is the thickness of the nonconducting flaw.

For the test situation, a=3 inches, the coil diameter is reasonable, l=3 inches for the effective depth of penetration is reasonable, and t= 0.125 inches or t= 0.394 inches depending on void inhomogeneity test piece thickness.

5.2 Surface Inhomogeneity Measurement Interpretation

The interpretation of the EMI signal will depend on the amplitude of the EMI signal. The amplitude can be compared to predictions. The lower conductivity tests were dominated by the distance from the surface that the MIZ-40A was 'zeroed.' The higher conductivity tests are more strongly affected by the medium electrical conductivity. The 40 mS/cm test is the most sensitive to the surface inhomogeneity effect on EMI signal amplitude because the electrical conductivity is the highest.

Figures in the Appendix portray the measured amplitude and phase for the surface inhomogeneity tests. There is no inhomogeneity effect on EMI signal phase, as expected. The inhomogeneity effect on EMI signal amplitude is compared to inhomogeneity surface area calculations are shown in Table 1.

The data in Table 1. has several items for discussion. First, the EMI probe was "zeroed" at different distances from the electrically conductive medium. This introduced some differences in measured signal amplitudes that were not caused by surface inhomogeneities. The calculated reduction of EMI signal amplitude was simply calculated from the formula given at the end of the previous section for a non-conducting disk inhomogeneity with a transverse EMI field.

W part and X part (dimensions in inches):

$$Amplitude\ Reduction \approx \frac{(Sampled\ Volume) - (Inhomogeneity\ Volume)}{Sampled\ Volume}$$

$$= \frac{((\pi/4)*(a^2)*h) - (t*a*h)}{(\pi/4)*(a^2)*h} = \frac{(\pi/4)*a - t}{(\pi/4)*a}$$

$$= \frac{(2.356) - (0.394)}{2.356} = 0.8328$$

Table 1. EMI Surface Inhomogeneity Test Results
Measured versus Calculated EMI Signal Amplitudes
Inhomogeneities: None, W, X and Y
40 mS/cm Electrical Conductivity

Lift-off	320 khz	340 khz	360 khz	
None				
-1.438	0.09756	0.1088	0.1419	
0	4.572	5.344	5.695	
W				
-2.018	0.05629	0.09062	0.09121	
0	3.597	4.220	4.508	
% Measured	0.786745	0.789671	0.791572	
% Calculated	0.832781	0.832781	0.832781	
Ratio	0.94472	0.948233	0.950516	0.947823
X				
-4.101	0.1553	0.1525	0.1486	
0	3.957	4.601	4.854	
% Measured	0.865486	0.860966	0.852327	
% Calculated	0.832781	0.832781	0.832781	
Ratio	1.039271	1.033844	1.02347	1.032195
Y				
-2.337	0.07718	0.08551	0.08192	
0	4.425	5.191	5.456	
% Measured	0.967848	0.97137	0.958033	
% Calculated	0.946948	0.946948	0.946948	
Ratio	1.02207	1.02579	1.011706	1.019855

The ratio rows calculated in Table 1 are the ratio of measured to calculated EMI amplitude reduction with volume inhomogeneity. Average ratios tabulated in Table 1 with values close to 1.0 are consistent with EMI signal proportional to the void inhomogeneity fraction not contributing to sampled volume electrical conductivity.

Y part (dimensions in inches):

$$\textit{Amplitude Reduction} \approx \frac{(\textit{Sampled Volume}) - (\textit{Inhomogeneity Volume})}{\textit{Sampled Volume}}$$

$$= \frac{((\pi/4)*(a^2)*h) - (t*a*h)}{(\pi/4)*(a^2)*h} = \frac{(\pi/4)*a - t}{(\pi/4)*a}$$

$$= \frac{(2.356) - (0.125)}{2.356} = 0.9469$$

This volume calculation assumes that the inhomogeneity depth is at least equal to the EMI depth of interrogation. This was expected because the 90% depth of interrogation is approximately 3 inches and the inhomogeneity test pieces are 1.97 inches and 3.94 inches deep.

There was not adequate data to define the depth effect, but this is expected to be consistent with EMI depth sensitivity, that about 90% of the EMI signal is from the top 3 inches.

Another way to state this conclusion is that the EMI signal is proportional to the effective density of the medium, that is the medium density and inhomogeneities the space occupied by voids. The final effect due to void inhomogeneities under the EMI probe is that the EMI inferred moisture content assuming no void inhomogeneities will be a lower limit for the actual moisture content of the same solid with void inhomogeneities actually present.

Table 2 shows the EMI inferred moisture content for different void fractions that reduces the effective medium density by (1.-void fraction). The actual moisture content necessary to give a certain measured electrical conductivity is tabulated in the column under the void fraction assumed.

Table 3 shows the difference between moisture content with known void fractions and the EMI inferred moisture content assuming zero void fraction. Table 3 also shows the ratio of moisture content with known void fractions to the EMI inferred moisture content assuming zero void fraction. The second part of Table 3 was used to estimate the EMI underestimate of the free water content assuming zero void inhomogeneities. Figure 4, Electrical Conductivity versus Moisture Content and subtitled Inhomogeneity Effect (Void Fractions), shows the Table 2 information in a graph.

6.0 REFERENCES

Burrows, M. L., 1964, *A Theory of Eddy-Current Flaw Detection*, Doctoral Dissertation, University of Michigan.

Wittekind, W. D., and R. D. Crowe, May 1996, *Electromagnetic Induction Probe Calibration for Electrical Conductivity Measurements and Moisture Content Determination of Hanford High Level Waste*, WHC-SD-ER-531 REV 0, Westinghouse Hanford Company, Richland, Washington.

Wittekind, W. D., R. D. Crowe, D. L. Lessor, and S. D. Tomich, October 1996, *Surface Moisture Measurement System Electromagnetic Induction Probe Characterization*, WHC-SD-WM-ER-606 REV 0, Westinghouse Hanford Company, Richland, Washington.

Table 2. Calculated EMI Moisture Content with Known Voids*					
Void Fraction	0.00	0.05	0.10	0.25	0.50
EMI Measured Electrical Conductivity mS/cm					
80	0.2678	0.2724	0.2772		
60	0.2429	0.2473	0.2519	0.2678	
40	0.2102	0.2142	0.2184	0.2331	0.2678
20	0.1611	0.1644	0.1680	0.1804	0.2102
10	0.1212	0.1238	0.1267	0.1367	0.1611
5	0.0897	0.0917	0.0940	0.1018	0.1212

*EMI moisture content calculated assuming: Porosity θ = 0.50; Interstitial liquid electrical conductivity σ_W = 200 mS/cm, Solid density ρ_S= 2.20 g/cm^3, Liquid density ρ_L= 1.177 g/cm^3, Proportion of water in interstitial liquid (ρ_{H2O}/ρ_L)= 0.792.

Table 3. Void Effect on EMI Inferred Moisture Content Difference Between EMI Moisture Content With Known Voids And EMI Moisture Content Without Voids					
Void Fraction	0.00	0.05	0.10	0.25	0.50
EMI Measured Electrical Conductivity mS/cm					
80	0.0000	0.0046	0.0094		
60	0.0000	0.0043	0.0090	0.0249	
40	0.0000	0.0040	0.0082	0.0229	0.0576
20	0.0000	0.0033	0.0069	0.0193	0.0490
10	0.0000	0.0027	0.0055	0.0155	0.0400
5	0.0000	0.0021	0.0043	0.0121	0.0315
Ratio of EMI Moisture Content With Known Voids To EMI Moisture Content Without Voids					
80	1.0000	1.0171	1.0352		
60	1.0000	1.0179	1.0369	1.1024	
40	1.0000	1.0190	1.0392	1.1092	1.2742
20	1.0000	1.0206	1.0426	1.1195	1.3043
10	1.0000	1.0219	1.0454	1.1280	1.3300
5	1.0000	1.0230	1.0477	1.1347	1.3509

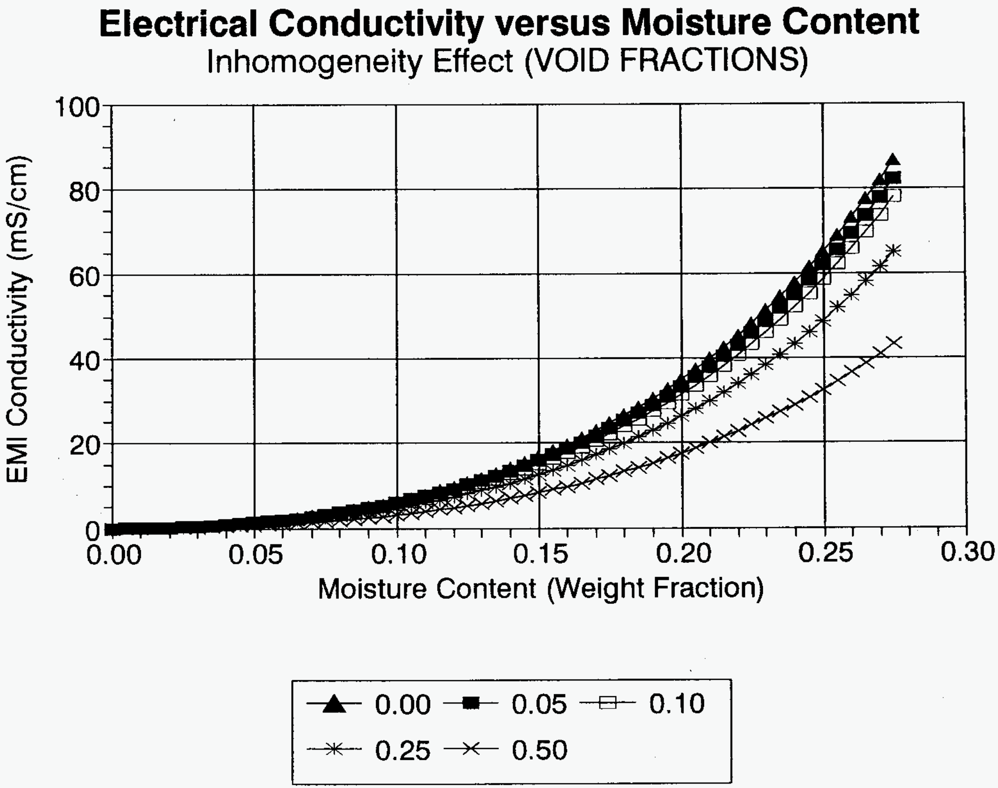

Figure 4. Electrical Conductivity versus Moisture Content Inhomogeneity Effect (Void Fractions)

APPENDIX

Figure A-1. Irregularity Effect 0 mS/cm - Amplitude

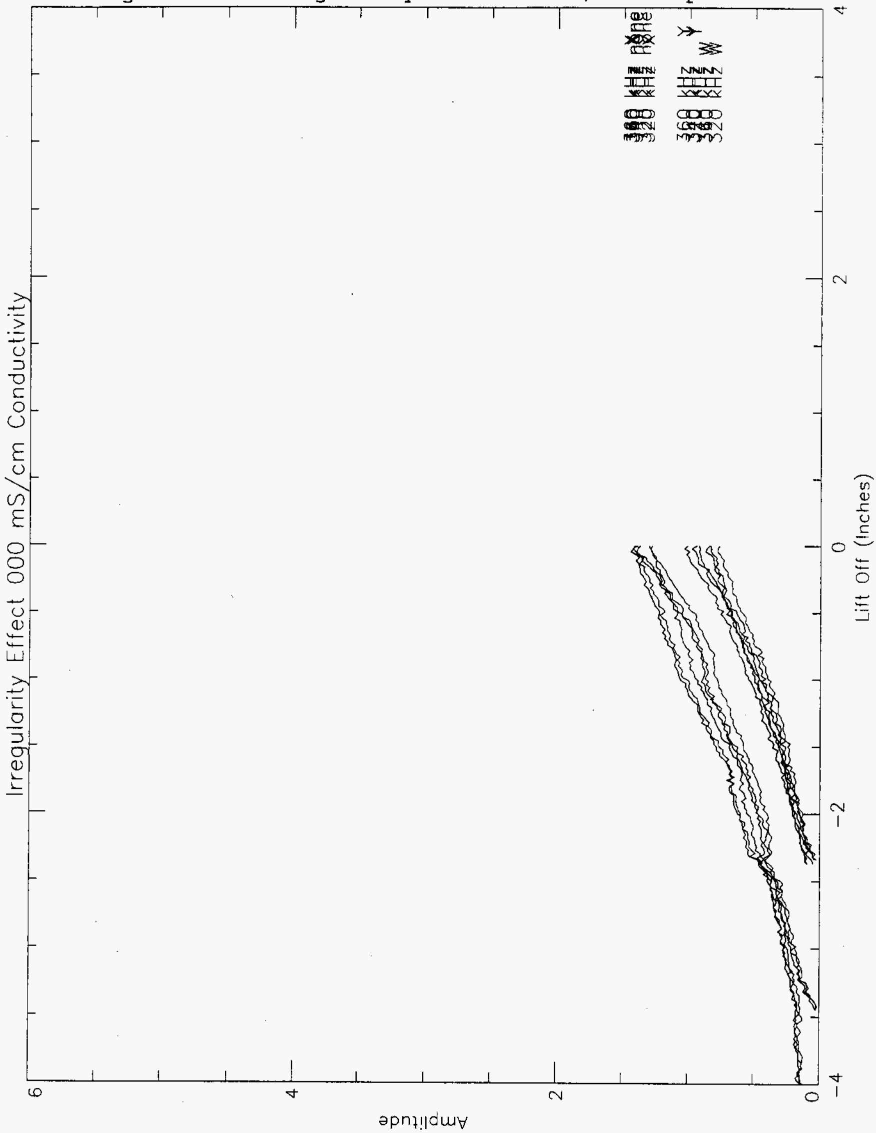

Figure A-2. Irregularity Effect 5 mS/cm - Amplitude

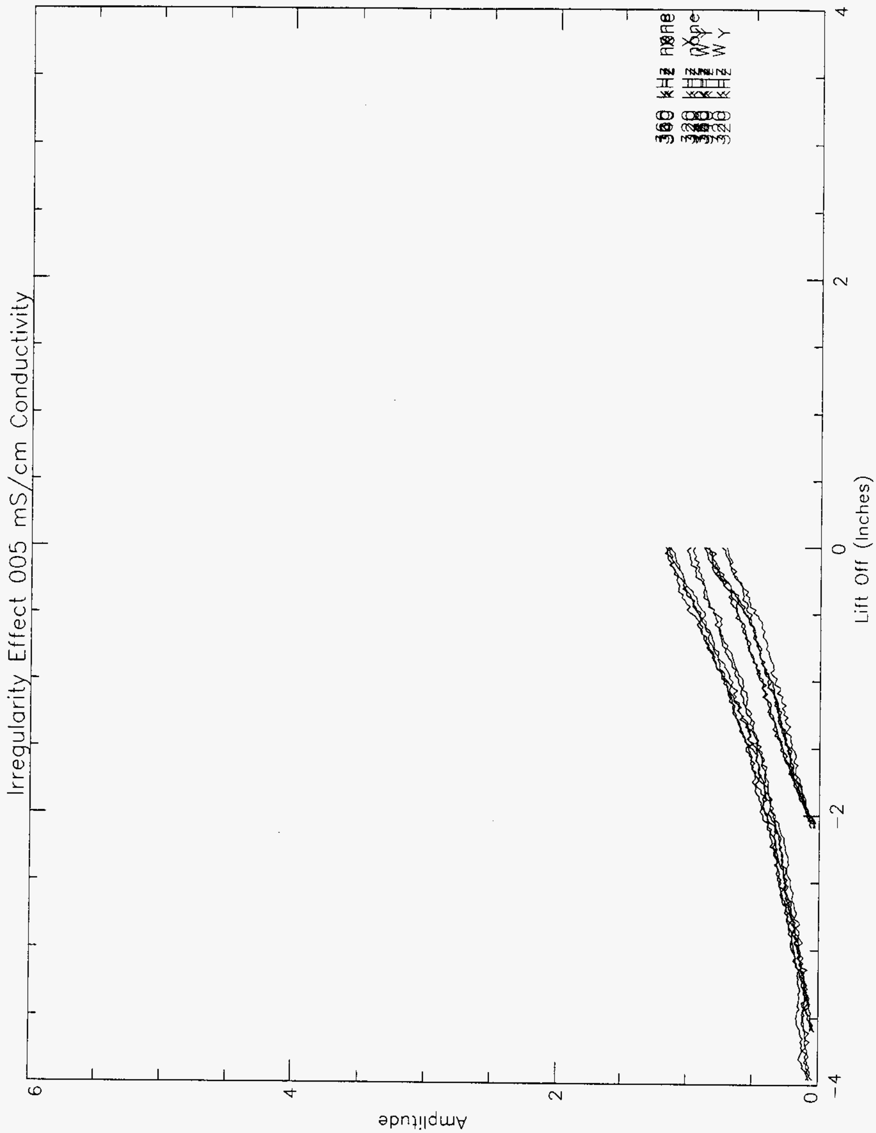

Figure A-3. Irregularity Effect 10 mS/cm - Amplitude

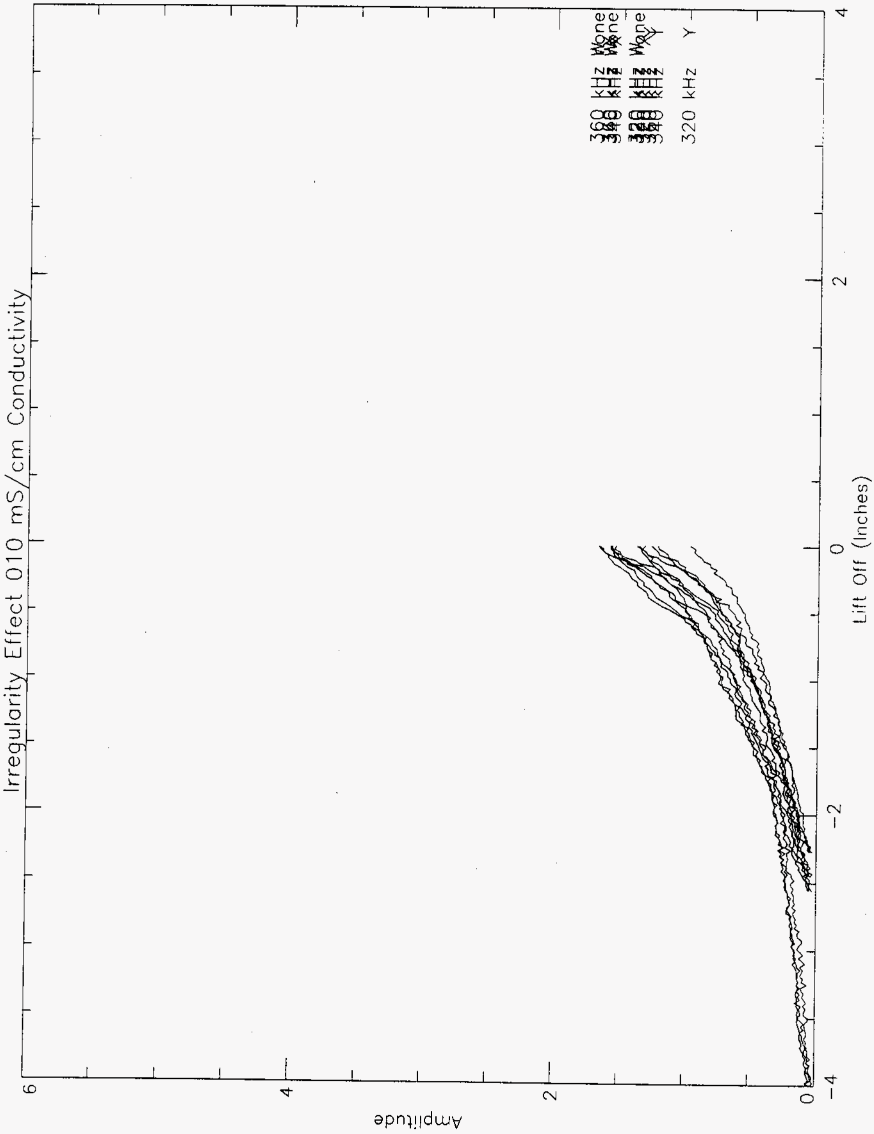

Figure A-4. Irregularity Effect 20 mS/cm - Amplitude

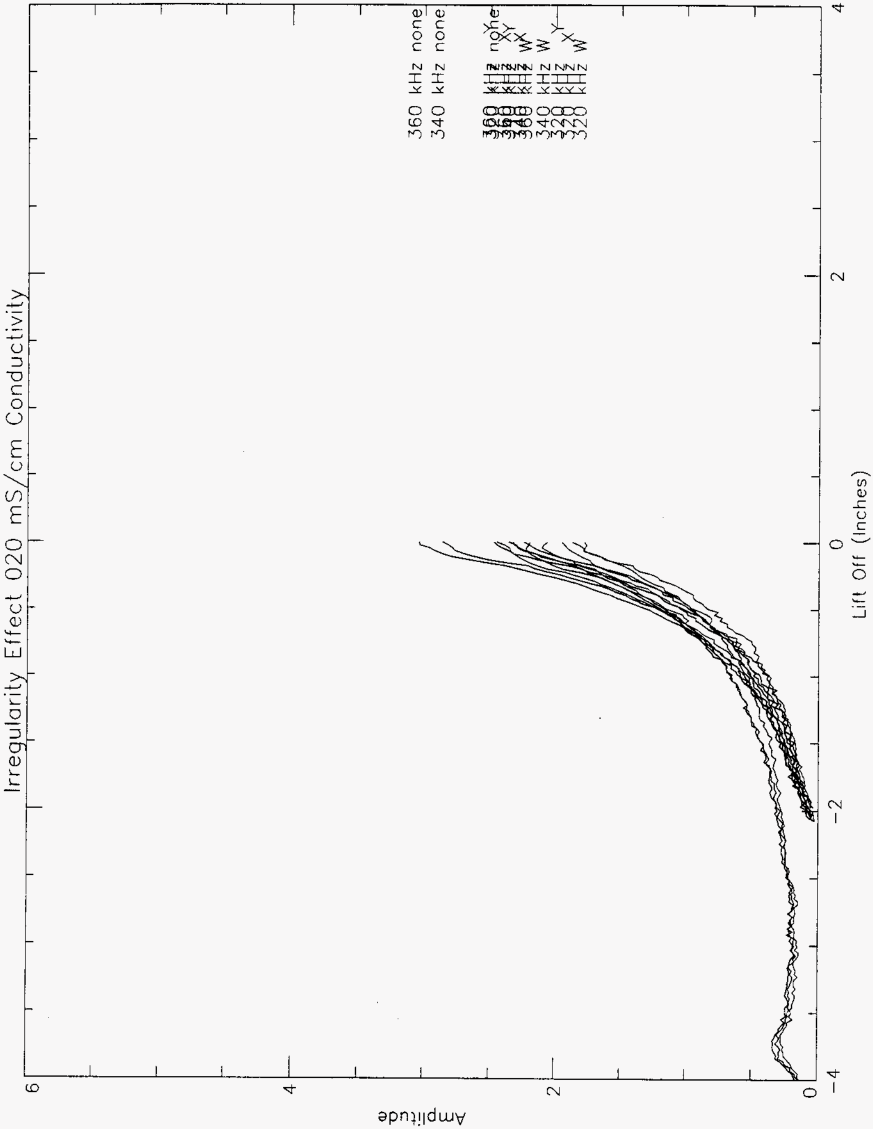

Figure A-5. Irregularity Effect 40 mS/cm - Amplitude

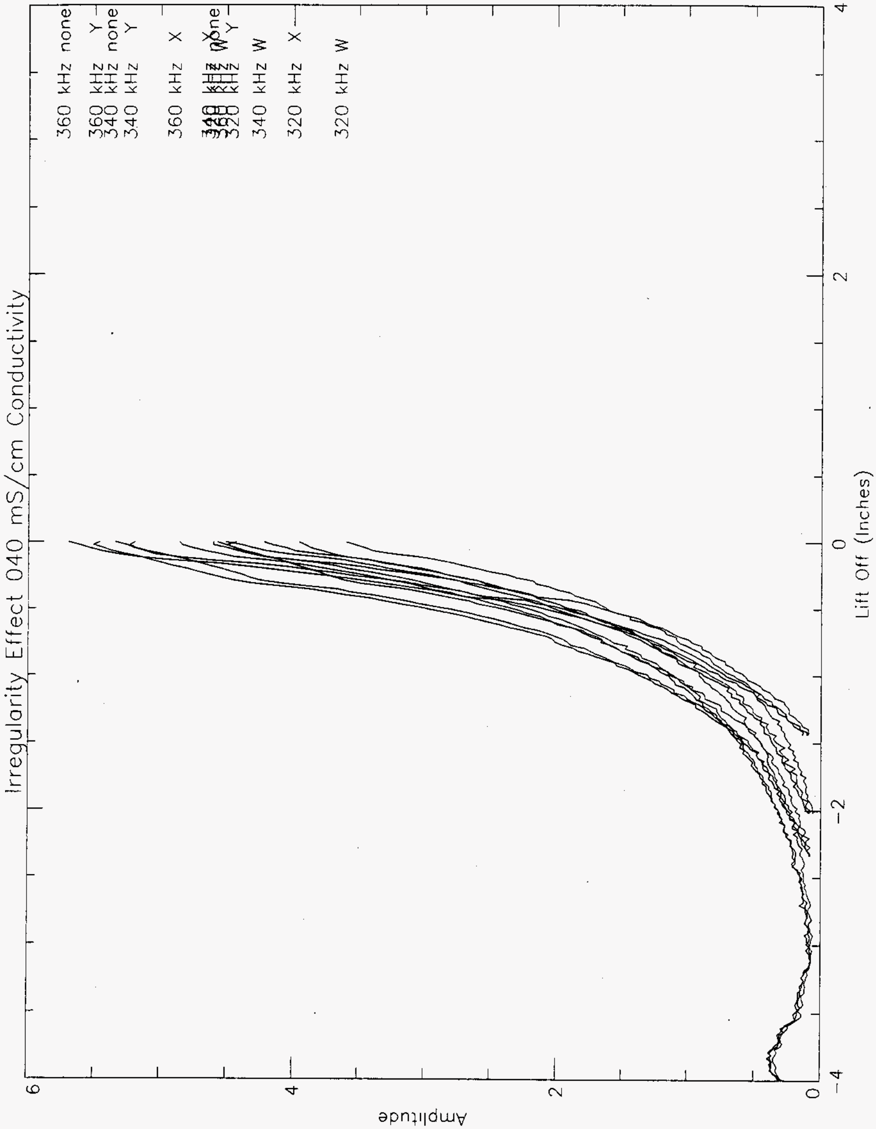

Figure A-6. Irregularity Effect 0 mS/cm - Phase

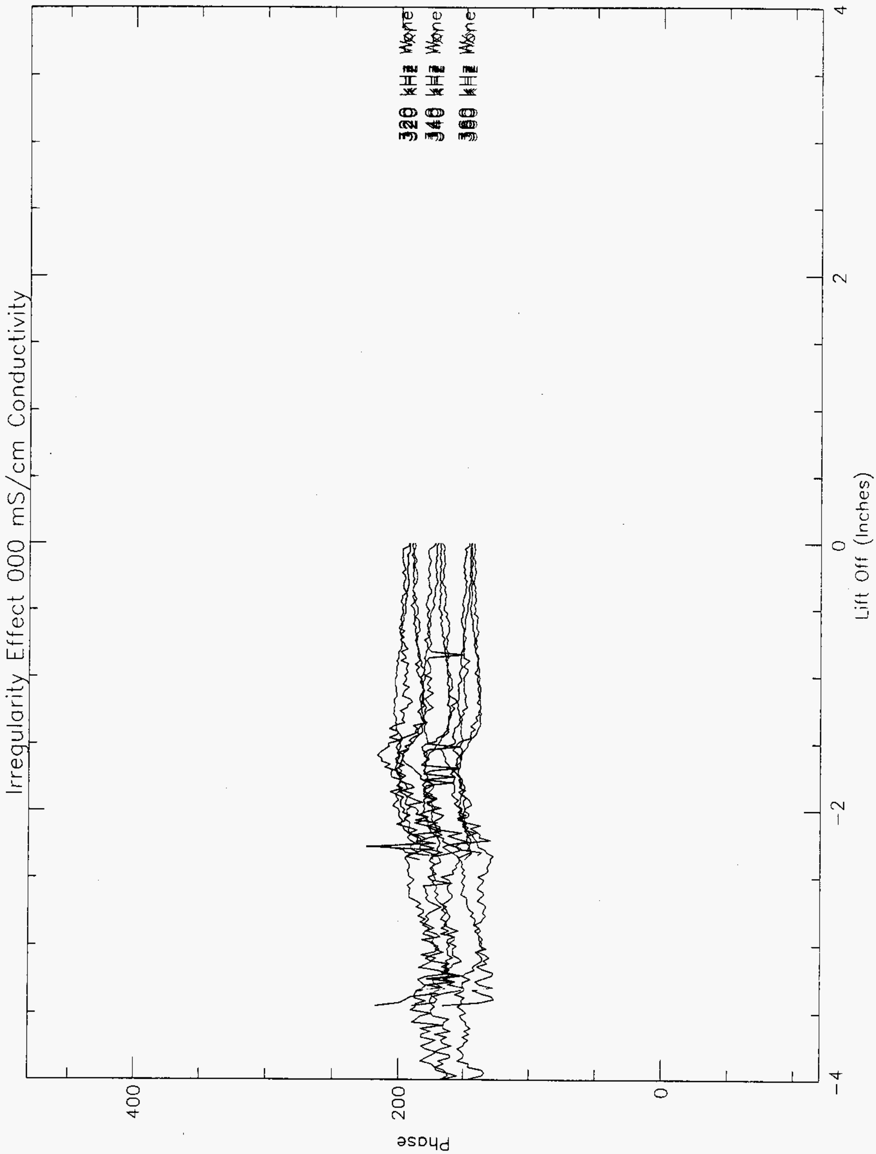

Figure A-7. Irregularity Effect 5 mS/cm - Phase

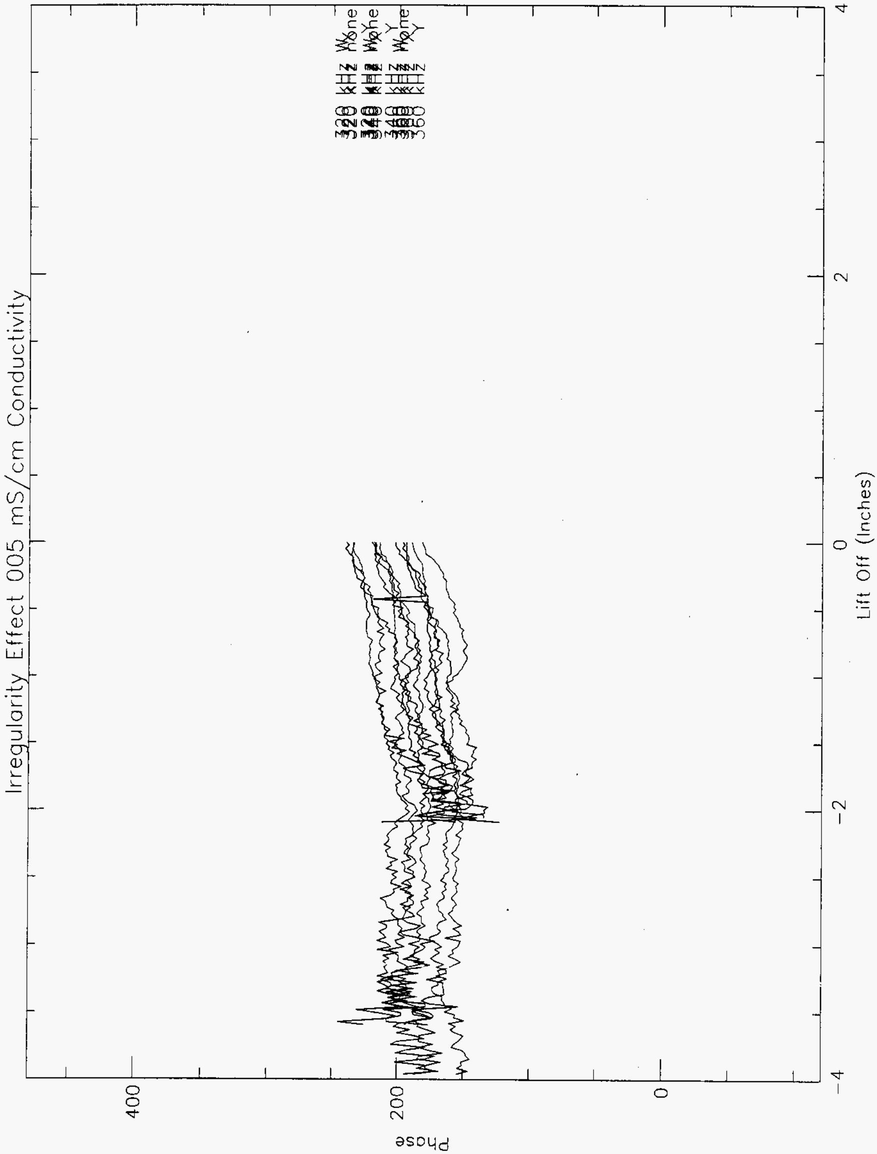

Figure A-8. Irregularity Effect 10 mS/cm - Phase

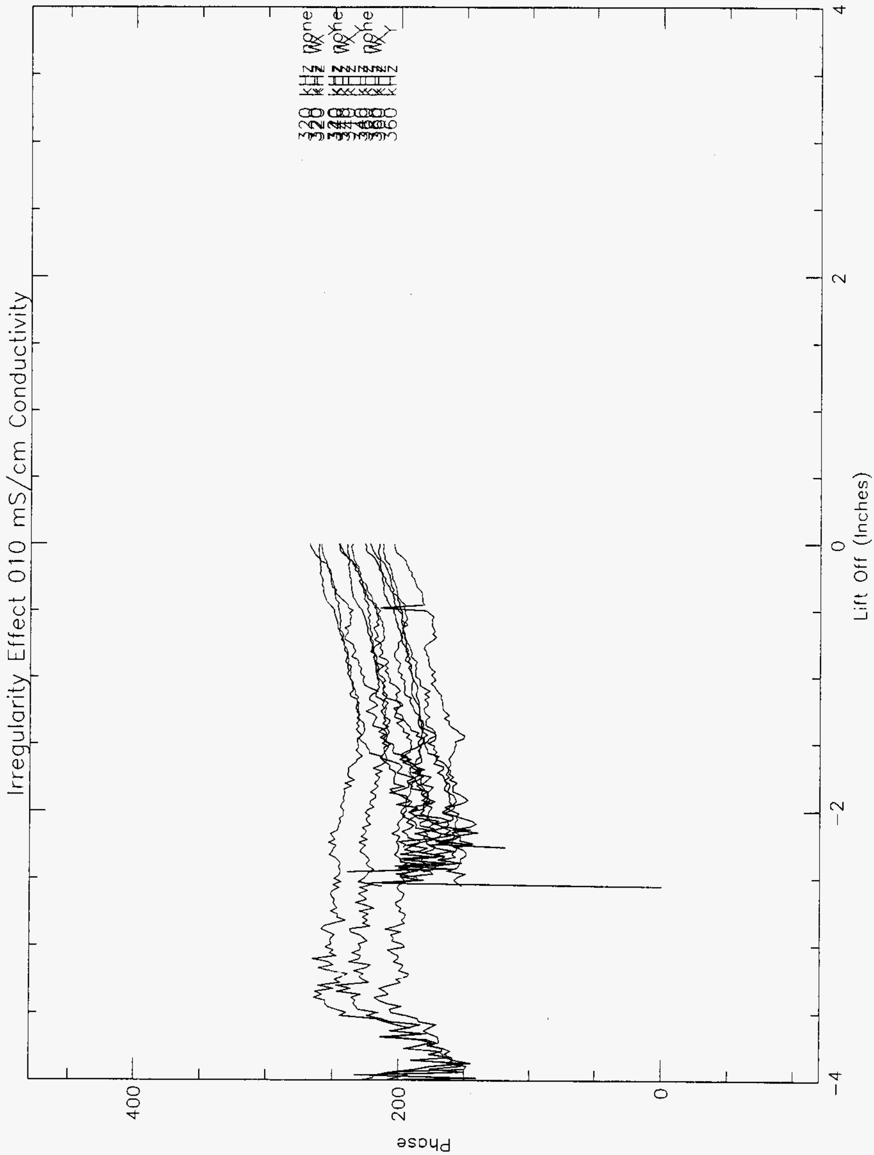

Figure A-9. Irregularity Effect 20 mS/cm - Phase

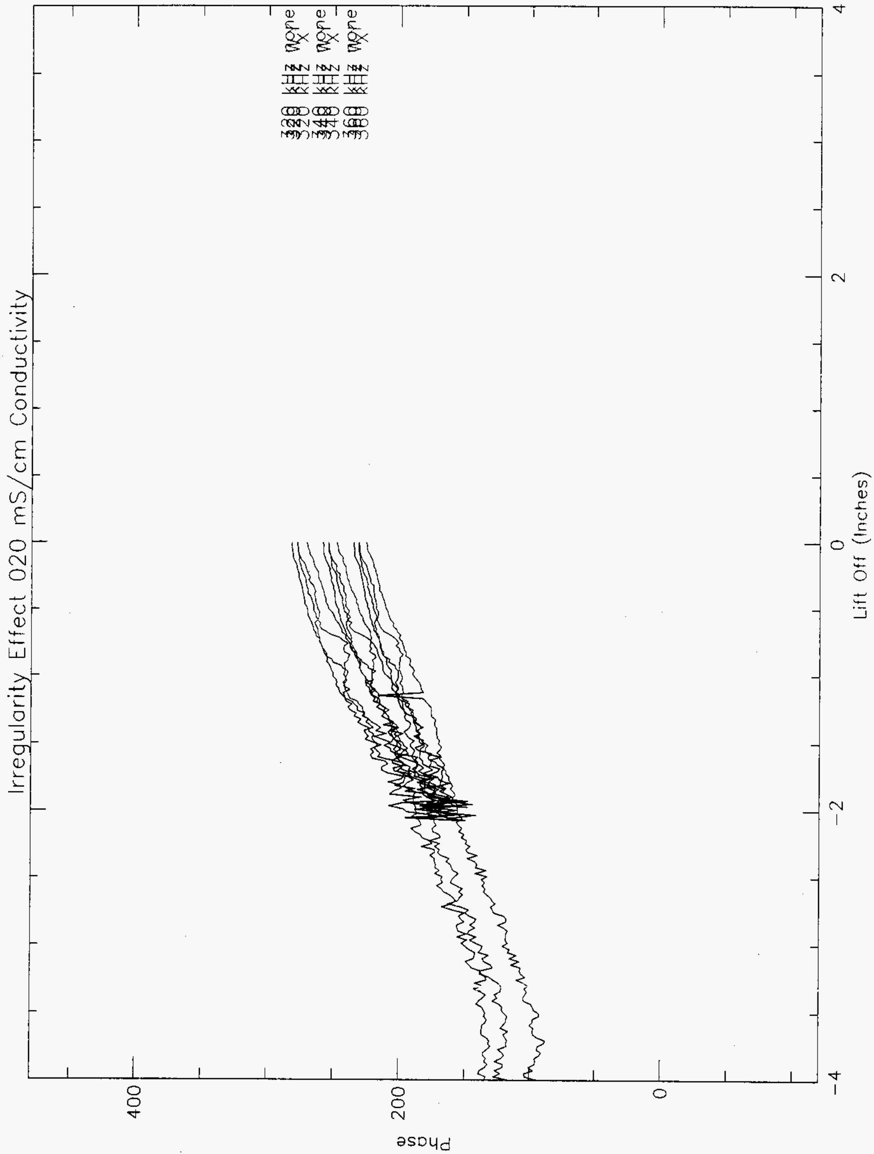

Figure A-10. Irregularity Effect 40 mS/cm - Phase

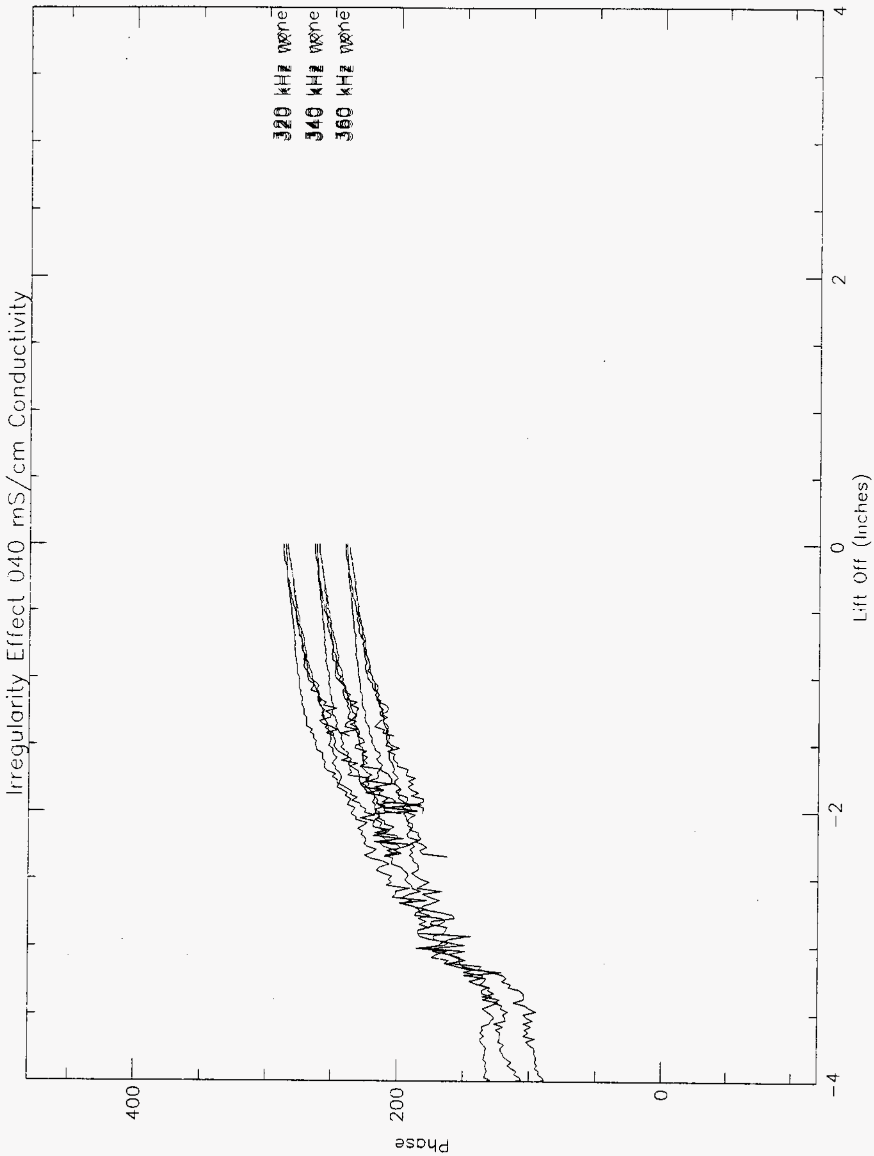

Figure A-11. Electrical Conductivity versus Moisture Content
Hanford Waste Tank Model

EMI moisture content calculated assuming: Porosity θ = 0.50; Interstitial liquid electrical conductivity σ_w = 200 mS/cm; Solid density ρ_s = 2.20 g/cm^3; Liquid density ρ_L = 1.177 g/cm^3; Proportion of water in interstitial liquid (ρ_{H2O}/ρ_L) = 0.792.

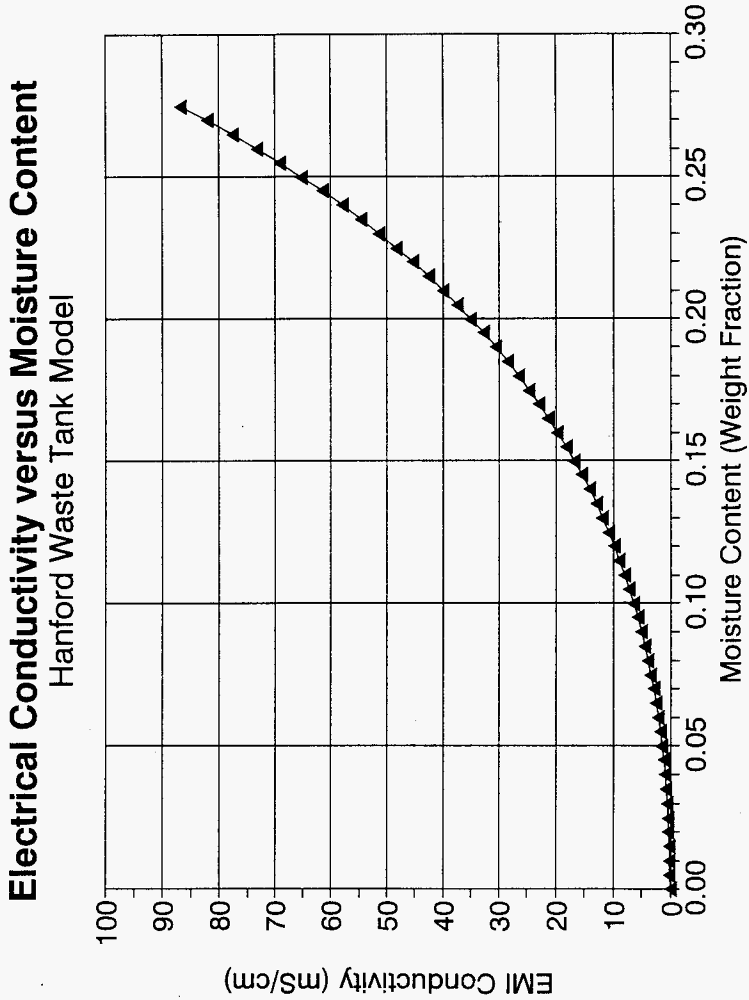

DISTRIBUTION SHEET

To	From	Page 1 of 1
Distribution	Criticality and Shielding	Date October 11, 1996
Project Title/Work Order		EDT No. 619216
Surface Moisture Measurement System Electromagnetic Induction Probe Surface Irregularity Tests		ECN No.

Name	MSIN	Text With All Attach.	Text Only	Attach./ Appendix Only	EDT/ECN Only
R. J. Cash	S7-14	X			
R. D. Crowe	A3-34	X			
K. L. Drury	H5-09	X			
G. T. Dukelow	S7-14	X			
J. Greenborg	H0-35	X			
D. L. Lessor	K7-15	X			
J. E. Meacham	S7-14	X			
E. R. Siciliano	H0-31	X			
T. I. Stokes	L6-37	X			
G. F. Vargo, Jr.	H5-09	X			
W. T. Watson	H0-31	X			
W. D. Wittekind	H0-35	X			
Central Files (Original +1)	A3-88	X			

A-6000-135 (01/93) WEF067